DE GRUYTER OPEN

Properties of thin ZnS:Mn films sprayed by improved method: The role of Mn^{2+} ion concentration

RANGNATH V. ZAWARE[1,*], RATAN Y. BORSE[2], BHIVA G. WAGH[3]

[1]Department of Physics, S.N. Arts, D.J.M. Commerce and B.N.S. Science College, Sangamner-422605, Ahmednagar, Maharashtra, India

[2]M.S.G. Arts, Science and Commerce College, Malegaon Camp-423105, Nasik, India

[3]K.S.K.W. Arts, Science and Commerce College, CIDCO, Nasik-422008, Maharashtra, India

Undoped and Mn-doped thin ZnS films were deposited on ordinary glass substrates at temperature of 450 °C by an improved spray pyrolysis (ISP) method. The ISP parameters, such as carrier gas flow rate, solution flow rate and substrate temperature, were controlled with accuracy ±0.25 Lpm, ±1 mL/h and ±1 °C, respectively. A pulse-spray mode of the method was used to spray the precursor solution. Thin film samples were prepared for Mn-doping with the concentrations of 0 at.%, 1 at.%, 3 at.%, 6 at.%, 8 at.% and 12 at.% relative to Zn in the spray solution. The Mn-doping concentration dependent chemical composition, surface morphology, and structural, optical and photoluminescence (PL) properties were studied. All the thin films were well adherent, nearly stoichiometric, dense, uniform, and possessed cubic crystal structure with preferential orientation along ⟨1 1 1⟩ direction. A slight enhancement in structural properties, an increase in band gap, and a decrease in refractive index and dielectric constant with Mn-doping concentration were observed. The PL spectra of Mn-doped thin ZnS films at room temperature exhibited both the 490 nm blue defect-related emission and the 590 nm yellow-orange Mn^{2+} ion related emission. The observed yellow-orange emission intensity was maximum for 3 at.% of Mn-doping concentration in the spray solution.

Keywords: *improved spray pyrolysis; pulse-spray mode; Mn-doped ZnS; Mn^{2+} ion concentration; photoluminescence*

1. Introduction

Zinc sulfide (ZnS) is one of the most important wide band gap semiconductors among the II-VI compound semiconductors. It has a wide range of applications including detectors, modulators, dielectric filters, light-emitting diodes, efficient phosphors in flat panel displays and buffer layers in solar cells [1, 2]. ZnS doped with various metals exhibit excellent luminescent properties when excited by X-rays, ultraviolet rays, cathode rays or electric current [3, 4]. Probably one of the most often studied materials for this purpose is manganese (Mn)-doped ZnS [5–9]. Zinc sulfide is a semiconductor suitable to be used as a host matrix for large variety of dopants because of its wide band gap [5, 6, 10]. The luminescent properties of ZnS doped with Mn have proved to be adequate for

electroluminescence applications. Mn is generally incorporated into the ZnS lattice as a Mn^{2+} ion in substitutional sites [9, 11]. The excitation and decay of Mn^{2+} ion produces a yellow-orange luminescence associated with transition between its $^4T_1$ and $^6A_1$ energy levels.

The most common techniques used for the deposition of zinc sulfide thin films are E-beam [9], molecular beam epitaxy [12], H$_2$ plasma chemical sputtering [13], MOVPE [14], MOCVD [15] and PLD [16]. Due to simplicity, low cost and capability to deposit optically smooth, uniform and homogeneous thin films over a large area, the conventional spray pyrolysis (CSP) technique has been widely used to deposit thin films for optoelectronic and photovoltaic applications. More recently, deposition of In, Al, Cu, and Mn-doped ZnS films using the spray pyrolysis technique have been reported [6, 17, 18]. In the previously reported literature, significant variation was observed

*E-mail: r.v.zaware@gmail.com

in the growth temperature, precursor ratio, dopant concentration, surface morphology and the optical properties of the films of desired quality; however, the reported results were found to be inconsistent. It could be due to embedded impurity, improper crystallinity and film non-uniformity, the effect of gravity and carrier gas flow rate on solution flow rate, etc., which may be attributed to the CSP technique [19]. In view of this, a spray pyrolysis technique has been improved and successfully employed for the deposition of high-quality thin ZnS films. In the present work, attempts have been made to deposit good-quality undoped and Mn-doped thin ZnS films by the improved spray pyrolysis (ISP) method. This paper reports the role of Mn^{2+} ion concentration in governing the properties of thin ZnS:Mn films sprayed by the improved method.

2. Experimental

2.1. Improved spray pyrolysis method

The ISP method that has been designed and developed for the deposition of thin films is reported elsewhere [20, 21]. This method has a good control over the carrier gas flow rate, solution flow rate and substrate temperature with accuracy ±0.25 Lpm, ±1 mL/h and ±1 °C, respectively. The rotameter, peristaltic pump and proportional-integral-derivative (PID) controller have been included in the CSP system to regulate and measure carrier gas flow rate, solution flow rate and substrate temperature, respectively. The solution flow rate was found completely free from the influence of the carrier gas flow rate and the gravity. A significant characteristics of the method is that the solution is sprayed in the form of pulses/packets at low peristaltic pump flow rate setting (<50 mL/h). A pulse-spray mode of the method may allow a sufficient time for the atoms to migrate and occupy vacant lattice sites, and thereby improve the quality of the deposited films.

2.2. Thin film deposition and characterization

The ISP setup, schematically shown in the Fig. 1, was used to deposit undoped and Mn-doped thin ZnS films. Double distilled water was used as a solvent to prepare the stock solutions of anhydrous zinc chloride ($ZnCl_2$), manganese chloride tetrahydrate ($MnCl_2 \cdot 4H_2O$) and thiourea ($SC(NH_2)_2$). 2.7258 g of zinc chloride (A.R. grade) was dissolved in 200 mL water to get 0.1 M basic solution. The basic solution of zinc chloride was cloudy due to presence of non-soluble zinc compounds [22]. A very small quantity of concentrated hydrochloric acid (HCl) was added into the basic solution so as to get a clean 0.1 M zinc chloride stock solution. 1.5224 g of thiourea (A.R. grade) was dissolved in 200 mL water to get its 0.5 M stock solution. Similarly, 1.979 g of manganese chloride tetrahydrate (A.R. grade) was dissolved in 100 mL water to get its 0.1 M stock solution. The stock solutions were filtered separately by filter paper before their use.

The precursor solution of molar Zn:S ratio of 1:5 was used to deposit thin ZnS films because the films deposited with this molar ratio were nearly stoichiometric [21, 23]. The solution of manganese chloride was used for doping of ZnS films with Mn^{2+} ions. The calculated amount of manganese chloride, zinc chloride and thiourea solutions were mixed together so as to get a precursor solution with the definite Mn-doping concentration, x. Ternary thin $Mn_xZn_{(1-x)}S$ films were synthesized with different Mn-doping concentrations: 0 at.%, 1 at.%, 3 at.%, 6 at.%, 8 at.% and 12 at.% relative to Zn in the spray solution. The films were deposited on an ordinary glass substrates of the size of 2.5 cm × 1 cm × 1.2 mm. The substrates were ultrasonically cleaned, washed with methanol and then dried under filtered air stream before use. Dry and clean compressed air with the flow rate of 10 Lpm was used to atomize the precursor solution. The peristaltic pump flow rate was set to 30 mL/h so as to spray the solution in the form of pulses. Actual solution flow rate dependent on tubing factor of the peristaltic pump was 0.9375 mL/min. In order to get uniformly distributed fine droplets of the solution over a larger cone area, the distance between the nozzle and the substrate was adjusted to 30 cm. For a good performance of the spray method it is known that the distance between a nozzle and

a substrate should be of the order of 25 cm to 35 cm [24]. Both nozzle and substrate were stationary during the film deposition. The undoped and Mn-doped thin ZnS films were prepared at optimized substrate temperature of 450 °C [20]. Two to three substrates were used at a time for each deposition cycle. Every time a 20 mL precursor solution was sprayed so as to avoid the effect of viscosity on its flow rate. ISP technique in a pulse-spray mode was used to deposit the films. As soon as the deposition was over, the heater was terminated and the films were allowed to cool naturally under the same process conditions. No further post-deposition heat treatment was employed to any of the films. The effect of Mn^{2+} ion concentration, x (at.%) on the composition, surface morphology, and structural and optical properties of these films was studied.
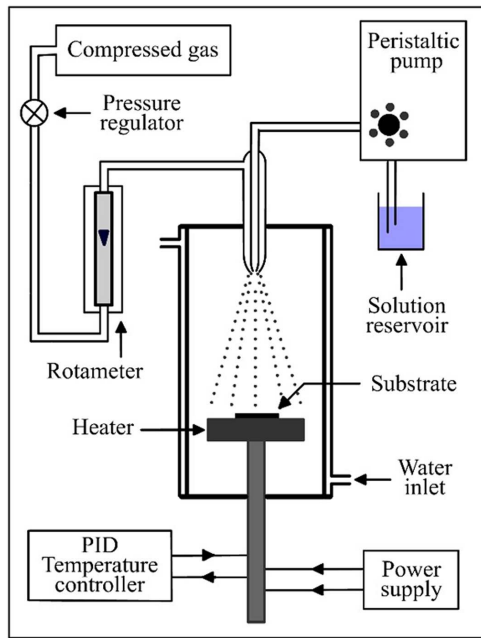

Fig. 1. Schematic diagram of the improved spray pyrolysis experimental setup.

X-ray diffraction measurements of the films were carried out using a diffractometer (Bruker AXS D8 ADVANCE XRD) with CuKα1 radiation. The surface morphology and chemical composition of the films were determined using FESEM (FEI NOVA Nano SEM-450) and SEM (JEOL, JED-2300) equipped with X-ray energy dispersive spectrometer (EDS). Film thickness was measured by gravimetric method. The optical absorption and transmission spectra for ZnS:Mn samples were obtained at room temperature using UV-Vis-NIR double beam spectrophotometer (JASCO, V-670). Their photoluminescence (PL) spectra were recorded at room temperature using a fluorescence spectrometer (PerkinElmer-LS) with a xenon lamp as an excitation source.

The crystallite size, D was calculated using Debye-Scherrer's formula [25, 26]:

$$D = \frac{k\lambda}{\beta \cos\theta} \qquad (1)$$

where β is the full width at half maximum (FWHM) of diffraction pattern, θ is the Bragg's angle, k is a constant taken as 0.9 and λ (1.5406 Å) is a wavelength of radiation used. The dislocation density, δ is defined as the length of dislocation lines per unit area of the crystal and was calculated using the formula [27]:

$$\delta = \frac{1}{D^2} \qquad (2)$$

The absorption coefficient, α of the films was obtained from an optical absorbance, A using the formula [28, 29]:

$$\alpha = \frac{2.303 \times A}{t} \qquad (3)$$

where t is the film thickness. The relation between the absorption coefficient, α and the energy of incident light, hν is given by [30]:

$$(\alpha h\nu)^p = B(h\nu - E_g) \qquad (4)$$

where B is a constant, E_g is the band gap energy, and p = 2 for direct band gap semiconductors, such as ZnS. The E_g for the films was estimated from a plot of $(\alpha h\nu)^2$ against incident photon energy (hν).

Refractive index, n for the ZnS:Mn films was determined using the formula [30]:

$$R = \frac{(n-1)^2}{(n+1)^2} \qquad (5)$$

where R is the reflectance.

The normal dielectric constant, ϵ of the thin films was estimated by [30]:

$$\varepsilon = n^2 - k^2 \quad (6)$$

where k is the extinction coefficient, which is given by [30]:
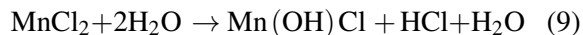
$$k = \frac{\alpha \times \lambda}{4\pi} \quad (7)$$

3. Results and discussion

3.1. Pyrolysis mechanism

In the experiment, precursors $MnCl_2$, $ZnCl_2$ and $SC(NH_2)_2$ were used as sources for Mn^{2+}, Zn^{2+} and S^{2-}, respectively. In the solution $ZnCl_2$ dissociates as [22]:
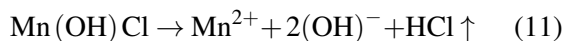
$$ZnCl_2 + 2H_2O \rightarrow Zn(OH)Cl + HCl + H_2O \quad (8)$$

Similarly, in the solution $MnCl_2$ dissociates as:

$$MnCl_2 + 2H_2O \rightarrow Mn(OH)Cl + HCl + H_2O \quad (9)$$

and at elevated temperature Zn(OH)Cl and Mn(OH)Cl decomposes as:

$$Zn(OH)Cl \rightarrow Zn^{2+} + 2(OH)^- + HCl\uparrow \quad (10)$$

and:

$$Mn(OH)Cl \rightarrow Mn^{2+} + 2(OH)^- + HCl\uparrow \quad (11)$$
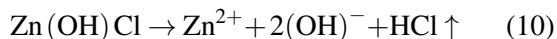
respectively.

The decomposition of thiourea is given in the literature [31], where:

$$CS(NH_2)_2 + 2(OH)^- \rightarrow S^{2-} + CN_2H_2\uparrow + 2H_2O\uparrow \quad (12)$$
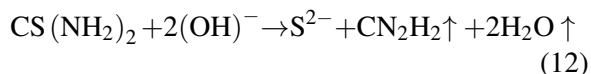
Finally, ZnS is formed according to the relation:

$$Zn_{(1-x)}^{2+} + Mn_x^{2+} + S^{2-} \rightarrow Mn_xZn_{(1-x)}S\downarrow \quad (13)$$
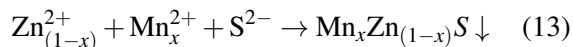
The byproducts CH_2N_2, H_2O and HCl formed during the pyrolytic decomposition, escape in a vapor form leaving behind the solid thin $Mn_xZn_{(1-x)}S$ film on a glass substrate.

3.2. Chemical composition and surface morphology

The chemical compositions of undoped and Mn-doped thin ZnS films were confirmed by energy dispersive spectroscopy (EDS). The EDS spectra for the thin films are not presented in this article. Chemical composition of the thin ZnS:Mn films was analyzed from a percentage by number of atoms (at.%) of elements Mn, Zn and S present in the thin films. The at.% of elements Si, Ca, O, Cl and C was not measured. A very small amount of oxygen, carbon and chlorine was observed in the ISP deposited thin ZnS films; it is analogous to our earlier reports [20, 21]. Table 1 shows initial at.% of Mn relative to Zn in the spray solution and content of elements Mn, Zn and S in the deposited films. In the spray solution, initial atomic percentage of S was 5 times higher than the one of Mn and Zn together. However, sulfur deficiency was observed in all the films. This may be due to the fact that sulfur has a great affinity towards oxygen, so it might have converted to SO_2 and then evaporated. In undoped ZnS, elements S and Zn were found in a near-stoichiometric (S/Zn = 0.91) ratio with a small sulfur deficiency (Zn = 52.47 at.%, S = 47.53 at.%). The (S/Zn) atomic ratio closer to 1 was reported for PLD-ZnS [32] and CBD-ZnS [33] thin films. The amount of Mn in the deposited films was found to increase from 0 at.% to 5.12 at.% with its doping concentration in the spray solution (Table 1). The EDS analysis also revealed that the chalcogen (S) to metal (Mn + Zn) ratio for the undoped and Mn-doped thin films was almost constant, so the as-deposited thin films were near-stoichiometric. The sprayed Cd-doped ZnS films [34], and Mn-doped ZnS nanoclusters [11, 35] with similar compositions have been reported. The content of elements Mn, Zn and S (Table 1) in each film indicates that the doping can be done very easily and effectively using ISP technique.

Surface morphology studies have been carried out on ZnS:Mn films deposited onto ordinary glass substrates at the deposition temperature of 450 °C. Fig. 2a and Fig. 2b are the representative micrographs (magnification of 150000×) of Mn-doped

Table 1. Initial atomic percentage (at.%) of Mn relative to Zn in the spray solution and final composition of Mn$_x$Zn$_{(1-x)}$S films.

Mn$_x$Zn$_{(1-x)}$S sample No.	Initial at.% of Mn relative to Zn in the spray solution		Final at.% of elements in the thin film by EDS analysis		
	Mn	Zn	Mn	Zn	S
1	0.00	100	0.00	52.47	47.53
2	1.0	99.0	0.39	52.21	47.4
3	3.0	97.0	1.38	51.31	47.31
4	6.0	94.0	2.59	50.67	46.74
5	8.00	92.0	3.85	49.58	46.57
6	12.00	88.0	5.12	48.57	46.31

thin ZnS films with doping concentrations of 3 at.% and 12 at.%, respectively. The Mn-doped thin films are observed to be dense and uniform in thickness and composition. In the films, the grains are agglomerated and the clusters so formed are of different geometries. Their average grain size determined by Cottrell method [36] and also by FESEM micrograph analysis was found to vary from 6 nm to 8 nm. The cluster boundaries are clearly observed in the micrograph for Mn-doping concentration equal to 12 at.% (Fig. 2b). It is also revealed that the surface microroughness of the films increases with the increase in Mn-doping.

3.3. Structural studies

II-VI chalcogenide semiconductor materials have good structural quality, and can be formed as either sphalerite (cubic) or wurzite (hexagonal) type [37]. The crystal structure of the Mn$_x$Zn$_{(1-x)}$S films was determined from the study of their X-ray diffraction patterns. The XRD patterns of undoped and Mn-doped thin ZnS films are shown in Fig. 3. The standard crystallographic data for MnS and ZnS compounds were taken from JCPDS Card #41-1049 and JCPDS Card #05-0566, respectively. The diffractograms of ZnS:Mn films reveal the presence of a prominent peak corresponding to (1 1 1) plane and other low intensity peaks corresponding to (2 2 0) and (3 1 1) planes of the material with cubic sphalerite crystal structure. The peaks corresponding to the planes (1 1 1), (2 2 0) and (3 1 1) were observed at Brag's angle of ∼28.68°, ∼47.77° and ∼56.6°, respectively.
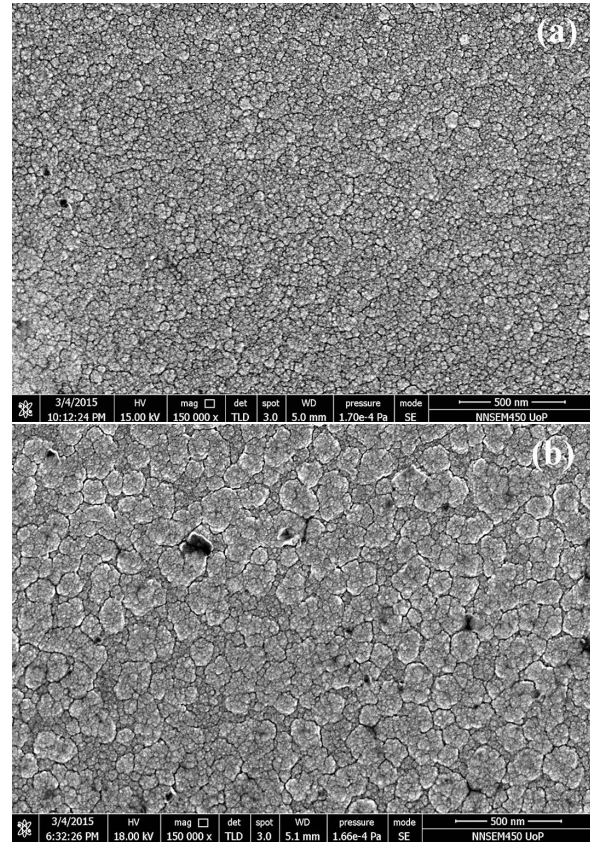

Fig. 2. FESEM micrographs of Mn-doped thin ZnS films: (a) 3 at.% and (b) 12 at.%.

No other diffraction peaks were detected except for ZnS related peaks. All the as-deposited undoped and Mn-doped thin ZnS films were polycrystalline. These results are in agreement with those of other authors [11, 35, 38, 39]. Moreover, a gradual increase in the intensity of the peak perpendicular

to the (1 1 1) plane shows that the crystallinity of the films was improved with Mn-doping concentration from 0 at.% to 12 at.%. The intensity of the (1 1 1) peak is greater for the ZnS:Mn film deposited with 12 at.% Mn concentration, which means that the texture of this film is better as compared to the other films. The estimated values of their lattice constant (a) were found to vary from 5.385 nm to 5.409 nm with Mn-doping concentration and are close to the reported values for cubic ZnS (JCPDS Card #05-0566, a = 0.5406 nm). It is observed that the incorporation of Mn leads to an increase in the lattice parameter (Table 2), hence, the unit cell size.

Average crystallites size of the film was estimated from the broadening of the diffraction pattern measured at half of its maximum intensity (FWHM). The FWHM of the diffraction curve corresponding to (1 1 1) plane was considered to determine the crystallites size. The crystallites size of the films was found to vary from 40 Å to 50 Å with the Mn-doping concentration. This has been ascribed to an improvement in the crystallinity and orientation of the crystals along a direction perpendicular to (1 1 1) plane (Fig. 3). In materials science, a dislocation is a crystallographic defect or irregularity within a crystal structure. The dislocation density in a crystal is defined as the average number of dislocation lines intersecting an area of 1 m^2 drawn within a body. The presence of dislocations strongly influences many of properties of materials [40]. The dislocation density estimated using equation 2 for all thin films was found to decrease from $6.14E^{+16}$ lines/m^2 to $3.99E^{+16}$ lines/m^2. With increasing Mn-doping concentration, the films turn out to be less defective.

3.4. Optical studies

It was observed that the thickness of the thin Mn$_x$Zn$_{(1-x)}$S film is dependent upon its Mn-doping concentration; the thickness was increased from 280 nm to 340 nm with Mn-doping concentration in the spray solution. All the films were thin. As the ionic radius of Mn^{2+} ions (0.80 Å) is larger than that of Zn^{2+} ion (0.74 Å), the increase in film thickness with Mn-doping concentration was
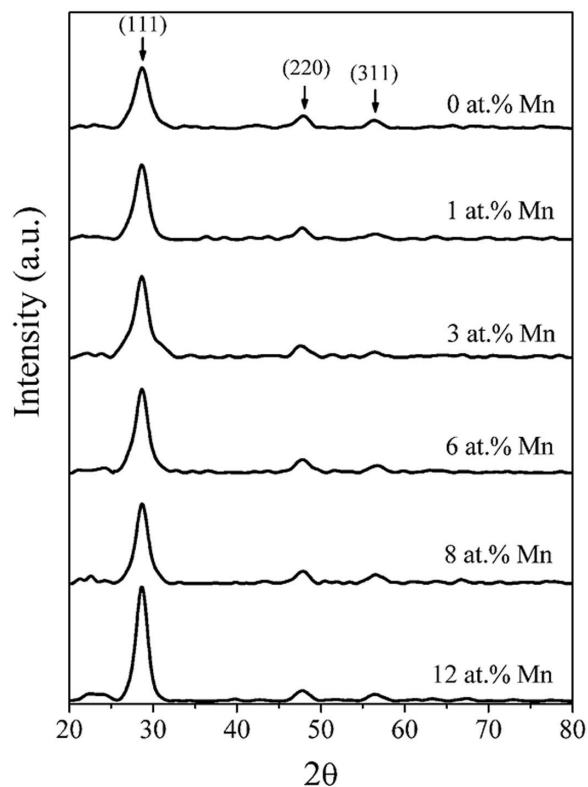

Fig. 3. XRD patterns of undoped and Mn-doped thin ZnS films.

clearly due to the substitution of Mn^{2+} ions in Zn^{2+} ion sites. It is well known that cubic ZnS is a direct band gap semiconductor [39]. The absorption and transmittance spectra of the Mn$_x$Zn$_{(1-x)}$S films deposited with Mn-doping concentrations of 0 at.%, 1 at.%, 3 at.%, 6 at.%, 8 at.% and 12 at.% were recorded in the photon energy range of 0.8266 eV to 6.1995 eV (wavelength range of 200 nm to 1500 nm). The absorption and transmittance spectra of undoped and Mn-doped ZnS samples are shown in the Fig. 4 and Fig. 5, respectively.

The optical absorption edges for the thin ZnS:Mn films are stiff (Fig. 4), which indicates that the thin films deposited by ISP method are composed of crystallites almost similar in shape and crystallites size, and the distribution of the constituents is homogeneous. The optical studies revealed that all the thin films are highly absorptive at about 312 nm. The linear nature of the plots at

Table 2. Lattice parameter (a), FWHM (β), crystallites size (D), band gap energy (E$_g$), refractive index (n), and dielectric constant (ε) of undoped and Mn-doped thin ZnS films prepared by the ISP method.

Mn$_x$Zn$_{(1-x)}$S sample No.	a [nm]	β [degree]	D [Å]	E$_g$ [eV]	n**	ε**
1	5.385	2.0317	40.36	3.610	2.53	6.41
2	5.386	1.8741	43.75	3.624	2.51	6.31
3	5.389	1.8892	43.41	3.632	2.49	6.22
4	5.400	1.8892	43.40	3.640	2.44	5.98
5	5.403	1.7401	47.12	3.652	2.41	5.81
6	5.409	1.6372	50.08	3.664	2.19	4.79

**Calculated at 546 nm (∼2.271 eV)

the absorption edge confirms that Mn$_x$Zn$_{(1-x)}$S is a semiconductor with a direct band gap [41]. ZnS has good absorption of light in the wavelength range of 220 nm to 350 nm [42]. From Fig. 6 it can be noted that the absorption edge is slightly shifted towards the high energy side with increasing Mn-doping concentration. The same shift of the absorption edge with increasing Mn-doping concentration up to 1.0 at.% at a fixed size of ZnS nanoclusters synthesized by hydrothermal process was reported in reference [11]. The transmittance of all the thin films was nearly 82 % in the visible range.
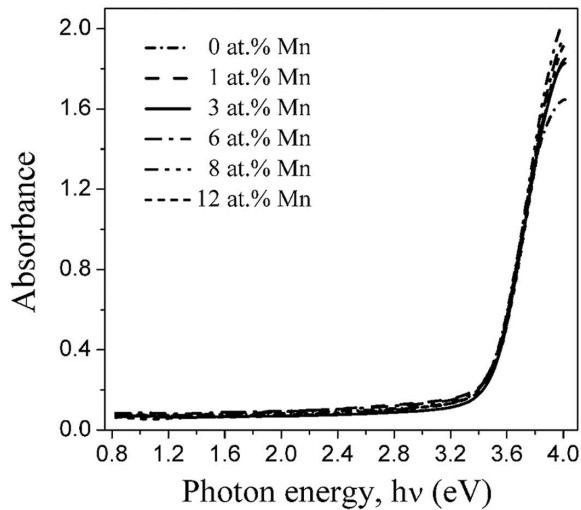

Fig. 4. Absorbance spectra of the undoped and Mn-doped thin ZnS films obtained by ISP technique.

The plots of square of (αhυ) versus hυ for the undoped and Mn-doped ZnS thin films are presented in Fig. 6. The band gap of the films was
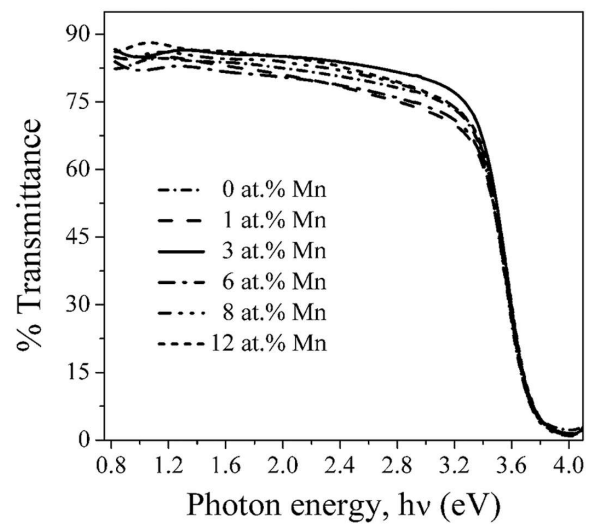

Fig. 5. Transmittance spectra of the undoped and Mn-doped thin ZnS films obtained by ISP technique.

determined by extrapolating a linear portion of the plot to x axis that corresponds to α = 0. The band gap of the thin Mn$_x$Zn$_{(1-x)}$S films was found to increase from 3.61 eV to 3.664 eV with Mn-doping concentration in the spray solution (Table 2). These values of band gaps can be compared with the band gap value of 3.6 eV for bulk ZnS at room temperature [43]. Hoa et al. [11] have also reported similar observations for Mn-doped ZnS nanoclusters with increasing Mn-doping concentration from 0.5 at.% to 3 at.%. Interestingly, the variation of the band gap is similar to what has been observed in case of Mn-doped CdS nanoclusters [44] and is opposite to what has been observed in case of Cd-doped thin ZnS sprayed films and Mn-doped ZnS nanocrystals [34, 45]. The increase in band gap of Mn-doped

thin ZnS film with increasing Mn concentration from 1 at.% to 12 at.% has been ascribed to sp-3d exchange interaction in a confined regime [11]. It has also been observed that a small amount of Mn present in the films greatly affects the optical band gap of ZnS. In an initial stage of Mn incorporation, the change in the band gap energy is large but later on, the change is small. This change in the band gap suggests that there is a direct energy transfer between semiconductor (host material) excited states and 3d levels of Mn^{2+} ions [46]. The transfer of energy is in the form of photogenerated carriers.
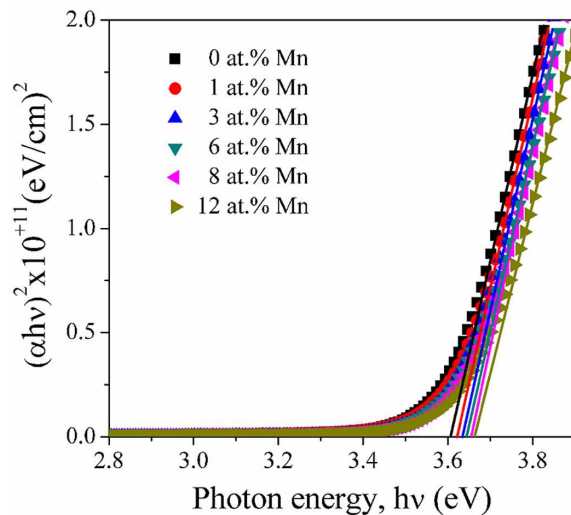

Fig. 6. Square of ($\alpha h\nu$) vs. incident photon energy ($h\nu$) plots for thin $Mn_xZn_{(1-x)}S$ films.

The diffuse reflectance spectra of the thin $Mn_xZn_{(1-x)}S$ films were recorded in the photon energy range of 1.55 eV to 3.00 eV (wavelength range of 400 nm to 800 nm). Fig. 7 shows the diffuse reflectance spectra of the undoped and Mn-doped thin ZnS films. In case of ISP prepared ZnS:Mn samples there was almost no change in absorbance (Fig. 4), but a considerable increase in transmittance (Fig. 5) and a decrease in reflectance (Fig. 7) in the visible region with Mn-doping concentration. Such behavior may be caused by all or one of the reasons: an increase in the thickness (so as the sample could fulfill the condition for antireflective coatings), reduction of the electrical conductivity and increase in microroughness
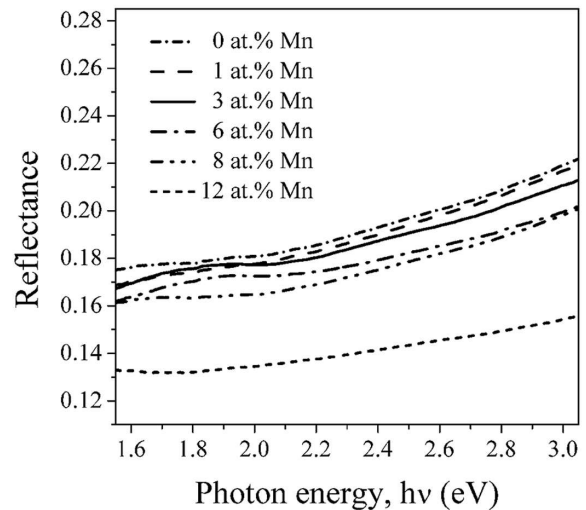

Fig. 7. Reflectance spectra of the undoped and Mn-doped thin ZnS films obtained by ISP technique.

of the sample surface with Mn-doping concentration [47]. The refractive index, n and the dielectric constant, ϵ of all the thin ZnS:Mn films were calculated using equation 5 and equation 6, respectively. Apart from increasing crystallites size and band gap energy, the n and ϵ were found to decrease from 2.53 eV to 2.19 eV and 6.41 eV to 4.79 eV, respectively, due to the decrease in optical reflectance of the thin films with the Mn-doping concentration (Fig. 7). The variations of n and ϵ with Mn-doping concentration are shown in Table 2. This type of behavior was not observed for previously reported Mn-doped ZnS films or ZnS nanoclusters. Apart from affecting the crystallinity, the increase in band gap energy and the decrease in refractive index of sputtered nanocrystalline thin ZnO films with Al ion-doping have been reported in the literature [48].

3.5. Photoluminescence studies

Fig. 8 shows the room temperature PL spectra excited with the radiation of energy $\sim$3.425 eV ($\lambda = 362$ nm) for the undoped thin ZnS film and the thin ZnS films doped with various Mn-doping concentrations 1 at.%, 3 at.%, 6 at.%, 8 at.% and 12 at.% in the spray solution. The amount of solution sprayed was 20 mL and the deposition time was 15.45 min for all the samples. It is observed

that the PL spectrum of the undoped sample shows only one dominant blue emission band centered at ~2.53 eV (λ = 490 nm) and Mn-doped samples show two emission bands peaked at ~2.53 eV and ~2.10 eV (λ = 590 nm). The emission peak at ~2.10 eV is associated with the characteristic emission from Mn^{2+} luminescent centers, while the ~2.53 eV peak is most likely caused by the radiative recombination involving defect states in the deposited ZnS films [49–51]. The emission band peaked at ~2.53 eV can be interpreted as a donor-acceptor pair (DAP) emission (Fig. 10). Proper accommodation of Mn atoms at substitutional sites is essential to generate Mn^{2+} luminescent centers; Zn vacancies would be filled by Mn atoms. The ~2.10 eV emission band is attributed to $^4T_1 \rightarrow {}^6A_1$ transition within 3d shell of Mn^{2+} ion [11, 52, 53]. The intensity of the PL of the thin films peaked at ~2.53 eV is maximum initially and then decreases, while the intensity of the PL peaked at ~2.10 eV initially increases rapidly to the maximum and then decreases slowly with the increase in Mn concentration. The decrease in blue emission intensity (~2.53 eV) with Mn-doping concentration may be due to the energy transfer by photogenerated carriers from ZnS host to Mn^{2+} ions. The variation of yellow-orange emission (~2.10 eV) intensity is depicted in Fig. 9.

The emission intensity of the $^4T_1 \rightarrow {}^6A_1$ transition is maximum for the Mn-doping concentration equal to 3 at.% in the spray solution (Fig. 9), which is in good agreement with previous reports [8, 35]. At higher Mn-doping concentrations (>3 at.%), because of a quenching effect, the intensity of the ~2.10 eV (λ = 590 nm) peak starts to decrease slowly. The effect of Mn-doping concentration has also been reported previously [6, 54]. Although the exact mechanism for this quenching to occur is still a matter of controversy, it is generally accepted that the quenching of the luminescence is associated with interaction among Mn^{2+} ions at the nearest, the second nearest, and probably even at the third nearest neighbor sites.

The observed PL behavior of the Mn-doped ZnS films can be interpreted in two ways: (a) the Mn^{2+} ion related PL can be generated at energies
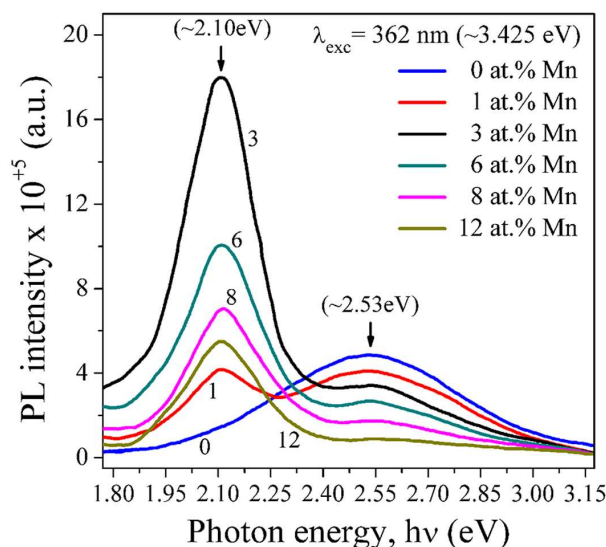

Fig. 8. The photoluminescence (PL) spectra of thin ZnS films with different Mn-doping concentrations in the spray solution.
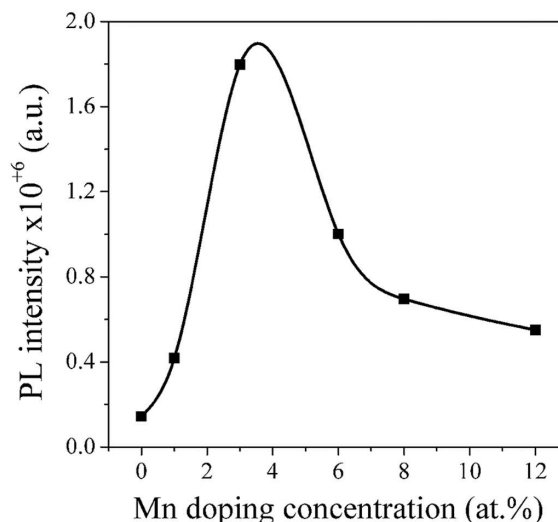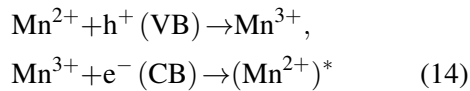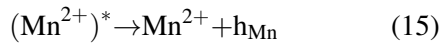

Fig. 9. Variation of yellow-orange emission (λ = 590 nm) intensity of thin ZnS:Mn films for different Mn-doping concentrations in the spray solution.

corresponding to Mn^{2+} ion own excited states, and (b) the electrons in the valence band of the ZnS host absorb the incident photon energy and transfer it to the conduction band, generating free electrons in the conduction band and free holes in the valence band (Fig. 10). At room temperature some of these photogenerated electrons and holes trapped

on the DAP states recombine, exhibiting the dominant blue emission. A number of the photogenerated holes in the valence band are trapped by Mn^{2+} ions which then become Mn^{3+} ions. The trapping of a number of the photogenerated electrons in the conduction band results in Mn^{2+} ions in an excited state $(Mn^{2+})^*$ and the following transitions of Mn ions from the excited state $(Mn^{2+})^*$ to the basic state (Mn^{2+}) come with the yellow-orange emission (Fig. 10). The process involved in it can be explained by the following equations [55]:

$$Mn^{2+}+h^+\,(VB) \rightarrow Mn^{3+},$$
$$Mn^{3+}+e^-\,(CB) \rightarrow (Mn^{2+})^* \qquad (14)$$

and:

$$(Mn^{2+})^* \rightarrow Mn^{2+}+h_{Mn} \qquad (15)$$

A part of the holes and the electrons just released from the DAPs are retrapped by Mn^{2+} ions, emitting the yellow-orange photon ($\sim$590 nm). The result is strong quenching of the blue emission, on the contrary, the intensity of the Mn^{2+} emission not only increases, but even to some extent, decreases with increasing Mn-doping concentration as observed in our ZnS:Mn samples.
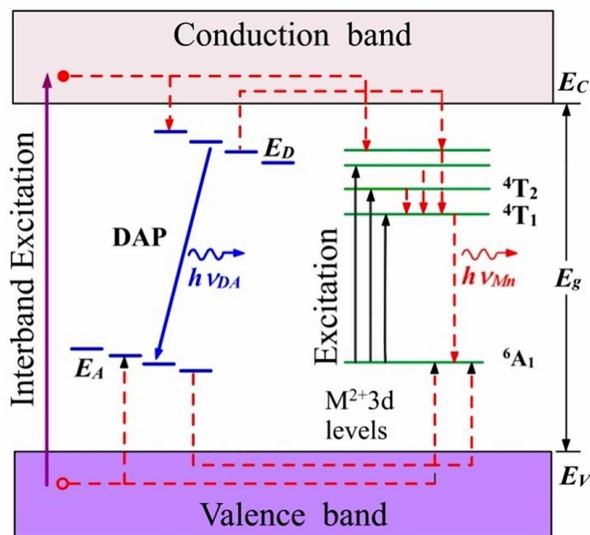

Fig. 10. Schematic representation of the mechanisms of photoluminescence (PL) excitation, energy transfer and PL in metal doped composites [11].

4. Conclusions

High-quality undoped and Mn-doped thin ZnS films were deposited at substrate temperature of 450 °C by an improved spray pyrolysis technique. The thin ZnS:Mn films were dense, fairly smooth and uniform. Extremely smooth films formation was possible by increasing their thickness. All the as-deposited thin films were polycrystalline with the cubic crystal structure with a lattice constant, a = 5.397±0.012 Å and the preferred orientation along the direction perpendicular to a (1 1 1) plane. The Mn content in the deposited thin film was found to increase from 0 at.% to 5.12 at.% with an increase in Mn-doping concentration from 0 at.% to 12 at.% relative to Zn in the spray solution. Consequently, the increase in thin film thickness from 280 nm to 340 nm and crystallites size from 4 nm to 5 nm was observed. The estimated band gap (3.61 eV), refractive index (2.53) and dielectric constant (6.41) of the undoped thin ZnS films were slightly higher than that of the bulk ZnS. Also an increase in band gap from 3.61 eV to 3.664 eV, a decrease in refractive index from 2.53 to 2.19 and dielectric constant from 6.41 to 4.79 with the Mn-doping concentration were observed. This kind of phenomenon is new and was not observed in the previously reported literature. The PL spectra of undoped thin ZnS film showed one peak at $\sim$2.53 eV (λ = 490 nm, blue emission) while Mn-doped thin films showed two peaks: one associated with the self-activated centre at $\sim$2.53 eV, and other at $\sim$2.10 eV (λ = 590 nm; yellow-orange emission) associated with the Mn^{2+} ions in ZnS films. Furthermore, the intensity of blue emission was dominant at 0 at.% and was found to decrease with the Mn-doping concentration. The yellow-orange emission intensity showed a maximum when the Mn-doping concentration was 3 at.%; the decrease in emission intensity for higher Mn-doping concentration was caused by quenching associated with interaction among neighboring Mn^{2+} ions. The thin ZnS films doped with Mn with 3 at.% concentration in the spray solution exhibited the best properties and behaved as efficient phosphor suitable for optoelectronic applications. The reported results will

be supportive to further developing ISP-ZnS:Mn technology.

Acknowledgements

References

[1] NAKAMURA S., YAMADA Y., TAGUCHI T., *J. Cryst. Growth*, 214 (2000), 1091.

[2] ELIDRISSI B., ADDOU M., REGRAGUI M., BOUGRINE A., KACHOUANE A., BERNEDE J.C., *Mater. Chem. Phys.*, 68 (2001), 175.

[3] QI L., LEE B.I., KIM J.M., JANG J.E., CHOE J.Y., *J. Lumin.*, 104 (2003), 261.

[4] WANG Z., DAEMEN L.L., ZHAO Y., ZHA C.S., DOWNS R.T., WANG X., WANG Z.L., *Nat. Mater.*, 4 (2005), 922.

[5] FALCONY C., *J. Appl. Phys.*, 72(4) (1992), 1525.

[6] BHISE M.D., KATIYAR M., KITAI A.H., *J. Appl. Phys.*, 67 (1990), 1492.

[7] ORTIZ A., GARCIA M., SANCHEZ A., FALCONY C., *J. Electrochem. Soc.*, 136 (1989), 1232.

[8] FALCONY C., ORTIZ A., DOMINGUEZ J.M., FARIAS M.H., COTA-ARAIZA L., SOTO G., *J. Electrochem. Soc.*, 139 (1992), 273.

[9] ROBBINS D.J., DIMARIA D.J., FALCONY C., DONG D.W., *J. Appl. Phys.*, 54 (1983), 4553.

[10] TANNAS L.E., *Flat Panel Displays and CRTs*, Van Nostrand, Reinhold, New York, 1985.

[11] HOA T.T.Q., THE N.D., MC VITIE S., NAM N.H., VU L.V., CANH T.D., LONG N.N., *Opt. Mater.*, 33 (2011), 308.

[12] TOMOMURA Y., KITAGAWA M., SUZUKI A., NAKAJIMA S., *J. Cryst. Growth*, 99 (1990), 451.

[13] TONOUCHI M., SUN Y., MIYASATO T., SAKAMA H., OHMURA M., *Jpn. J. Appl. Phys.*, 29 (1990), 2453.

[14] DEAN P.J., PITT A.D., SKOLNICK M.S., WRIGHT P.J., COCKAYNE B., *J. Cryst. Growth*, 59 (1982), 301.

[15] PORADA Z., SCHABOWSKA-OSIOWSKA E., *Thin Solid Films*, 145 (1986), 75.

[16] LUO P.F., JIANG G., ZHU C., *Chinese J. Chem. Phys.*, 22 (2009), 97.

[17] JONES G., WOODS J., *J. Lumin.*, 9 (1974), 389.

[18] SASAKURA H., KOBAYASHI H., TANAKA S., MITA J., TANAKA T., NAKAYAMA H., *J. Appl. Phys.*, 52 (1981), 6901.

[19] AFIFI H.H., MAHMOUD S.A., ASHOUR A., *Thin Solid Films*, 263 (1995), 248.

[20] ZAWARE R.V., WAGH B.G., *Mater. Sci.-Poland*, 32 (3) (2014), 375.

[21] ZAWARE R.V., WAGH B.G., *Arab. J. Sci. Eng.*, 40 (7) (2015), 2049.

[22] PEACOCK J.C., PEACOCK B.L.DEG., *J. Pharm. Sci.-US*, 7 (1918), 689.

[23] LOPEZ M.C., ESPINOS J.P., MARTIN F., LEINEN D., RAMOS-BARRADO J.S., *J. Cryst. Growth*, 285 (2005), 66.

[24] BOUBAKER K., CHAOUACHI A., AMLOUK M., BOUZOUITA H., *Eur. Phys. J. Appl. Phys.*, 37 (2007), 105.

[25] CULLITY B.D., STOCK S.R., *Elements of X-ray diffraction*, Prentice Hall, India, 2001.

[26] MURALI K.R., KUMARESAN S., *Chalcogenide Lett.*, 6 (2009), 17.

[27] VELUMANI S., MATHEW X., SEBASTIAN P.J., *Sol. Energ. Mat. Sol. C.*, 76 (2003), 359.

[28] ILICAN S., CAGLAR Y., CAGLAR M., *J. Optoelectron. Adv. M.*, 10 (2008), 2578.

[29] SHINDE M.S., AHIRRAO P.B., PATIL R.S., *Arch. Appl. Sci. Res.*, 3 (2011), 311.

[30] GOSWAMI A., *Thin Film Fundamentals*, New Age International Ltd., India, 2008.

[31] JOHNSTON D.A., CARLETTO M.H., REDDY K.T.R., FORBES I., MILES R.W., *Thin Solid Films*, 403 (2002), 102.

[32] LUO P.F., JIANG G., ZHU C., *Chinese J. Chem. Phys.*, 22 (2009), 97.

[33] LI Z.Q., SHI J.H., LIU Q.Q., WANG Z.A., SUN Z., HUANG S.M., *Appl. Surf. Sci.*, 257 (2010), 122

[34] RAVIPRAKASH Y., BANGERA K.V., SHIVKUMAR G.K., *Sol. Energy*, 83 (2009), 1645.

[35] FALCONY C., GARCIA M., ORTIZ A., ALONSO J.C., *J. Appl. Phys.*, 72 (1992), 1525.

[36] COTTRELL A., *An Introduction to Metallurgy*, University Press, Hyderabad, India, 2000.

[37] BOUROUSHIAN M., LOIZOS Z., SPYRELLIS N., MOURIN G., *Appl. Surf. Sci.*, 115 (1997), 103.

[38] BISWAS S., KAR S., *Nanotechnology*, 19 (2008), 45710.

[39] SAPRA S., NANDA J., ANAND A., BHAT S.V., SARMA D.D., *J. Nanosci. Nanotechno.*, 3 (2003), 392.

[40] TAYLOR G.I., *P. Roy. Soc. A-Math. Phy.*, 145 (1934), 362.

[41] XUANZHI W., *Sol. Energy*, 77 (2004), 803.

[42] JIANFENY C., YALING L., YUHONG W., JIMMY Y., DAPENG C., *Mater. Res. Bull.*, 39 (2004), 185.

[43] GENG B.Y., LIU X.W., DU Q.B., WEI X.W., ZHANG L.D., *Appl. Phys. Lett.*, 88 (2006), 163104.

[44] LEVY L., HOCHEPIED J.F., PILENI M.P., *J. Phys. Chem.*, 100 (1996), 18322.

[45] MOTE V.D., PURUSHOTHAM Y., DOLE B.N., *Ceramica*, 59 (2013), 614.

[46] BRIELER F.J., FROBA M., CHEM L., KLAR P.J., HEIMBRODT W., KRUG H.A., NIDDA V., LOIDL A., *Chem. Eur. J.*, 81 (2002), 185.

[47] DRIGGERS R.G. (Ed.), *Encyclopedia of Optical Engineering*, Vol. 3, CRC Press, India, 2003.

[48] MENDOZA-GALVAN A., TREJO-CRUZ C., LEE J., BHATTACHARYYA D., METSON J.B., EVANS P.J., PAL U., *J. Appl. Phys.*, 99 (2006), 1.

[49] KAR S., CHAUDHURI S., *J. Phys. Chem. B*, 109 (2005), 3298.

[50] ODA S., KUKIMOTO H., *J. Lumin.*, 18 – 19 (1979), 829.

[51] SAMELSON H., LEMPICKI A., *Phys. Review*, 125 (1962), 901.

[52] BHARGAVA R.N., GALLAGHER D., HONG X., NURMIKKO A., *Phys. Rev. Lett.*, 72 (1994), 311.

[53] LU H.Y., CHU S.Y., TAN S.S., *Jpn. J. Appl. Phys.*, 44 (7A) (2005), 5282.

[54] WARREN A.J., THOMAS C.B., STEWENS P.R.C., *J. Phys. D Appl. Phys.*, 16 (1983), 225.

[55] SUYVER J.F., WUISTER S.F., KELLY J.J., MEIJERINK A., *Nano Lett.*, 1 (2001), 429.